



GaAs High Breakdown Voltage Front and Back Side Processed Schottky Detectors for X-ray Detection

**by Fred Semendy, Satpal Singh, Mark Litz, Priyalal Wijewarnasuriya,
Kara Blaine, and Nibir Dhar**

ARL-TR-4308

November 2007

NOTICES

Disclaimers

The findings in this report are not to be construed as an official Department of the Army position unless so designated by other authorized documents.

Citation of manufacturer's or trade names does not constitute an official endorsement or approval of the use thereof.

Destroy this report when it is no longer needed. Do not return it to the originator.

Army Research Laboratory

Adelphi, MD 20783-1197

ARL-TR-4308**November 2007**

GaAs High Breakdown Voltage Front and Back Side Processed Schottky Detectors for X-ray Detection

**Fred Semendy, Satpal Singh, Mark Litz, Priyalal Wijewarnasuriya,
Kara Blaine, and Nibir Dhar**
Sensors and Electron Devices Directorate, ARL

REPORT DOCUMENTATION PAGE			<i>Form Approved</i> <i>OMB No. 0704-0188</i>		
Public reporting burden for this collection of information is estimated to average 1 hour per response, including the time for reviewing instructions, searching existing data sources, gathering and maintaining the data needed, and completing and reviewing the collection information. Send comments regarding this burden estimate or any other aspect of this collection of information, including suggestions for reducing the burden, to Department of Defense, Washington Headquarters Services, Directorate for Information Operations and Reports (0704-0188), 1215 Jefferson Davis Highway, Suite 1204, Arlington, VA 22202-4302. Respondents should be aware that notwithstanding any other provision of law, no person shall be subject to any penalty for failing to comply with a collection of information if it does not display a currently valid OMB control number. PLEASE DO NOT RETURN YOUR FORM TO THE ABOVE ADDRESS.					
1. REPORT DATE (DD-MM-YYYY) November 2007		2. REPORT TYPE Final		3. DATES COVERED (From - To)	
4. TITLE AND SUBTITLE GaAs High Breakdown Voltage Front and Back Side Processed Schottky Detectors for X-ray Detection			5a. CONTRACT NUMBER		
			5b. GRANT NUMBER		
			5c. PROGRAM ELEMENT NUMBER		
6. AUTHOR(S) Fred Semendy, Satpal Singh, Mark Litz, Priyalal Wijewarnasuriya, Kara Blaine, and Nibir Dhar			5d. PROJECT NUMBER		
			5e. TASK NUMBER		
			5f. WORK UNIT NUMBER		
7. PERFORMING ORGANIZATION NAME(S) AND ADDRESS(ES) U.S. Army Research Laboratory ATTN: AMSRD-ARL-SE-EI 2800 Powder Mill Road Adelphi, MD 20783-1197			8. PERFORMING ORGANIZATION REPORT NUMBER ARL-TR-4308		
9. SPONSORING/MONITORING AGENCY NAME(S) AND ADDRESS(ES) U.S. Army Research Laboratory 2800 Powder Mill Road Adelphi, MD 20783-1197			10. SPONSOR/MONITOR'S ACRONYM(S)		
			11. SPONSOR/MONITOR'S REPORT NUMBER(S) ARL-TR-4308		
12. DISTRIBUTION/AVAILABILITY STATEMENT Approved for public release, distribution unlimited.					
13. SUPPLEMENTARY NOTES					
14. ABSTRACT We have studied the current voltage and X-ray detection using front and back side processed, unintentionally doped bulk gallium-arsenic (GaAs) Schottky detectors and determined that GaAs detectors with a large enough thickness and low enough doping could be used for X-ray imaging, especially for medical applications. In this study, GaAs Schottky detectors were fabricated using front and back side photolithographic processing using Ti/Au for Schottky and Ge/Au/Ni/Au for ohmic contacts. A number of 2×2 mm detectors were tested. The breakdown voltage reached 600–800 V in semi-insulated (SI) GaAs Schottky front and back side processed detectors. For these detectors, the dark current was found to be between 2–90 nA. These detectors were also characterized with 150 keV, 3mA X-ray radiation and they responded well, showing more than a hundred fold increase in photocurrent due to production of electron hole pairs by the ionization processes. The processing of the detectors and the current-voltage (I-V) and X-ray characterizations are presented in this report.					
15. SUBJECT TERMS SI-GaAs, Schottky detectors, I-V characteristics, X-ray Detection					
16. SECURITY CLASSIFICATION OF:			17. LIMITATION OF ABSTRACT SAR	18. NUMBER OF PAGES 20	19a. NAME OF RESPONSIBLE PERSON Fred Semendy
a. REPORT U	b. ABSTRACT U	c. THIS PAGE U			19b. TELEPHONE NUMBER (Include area code) (301) 394-4627

Contents

List of Figures	iv
List of Tables	iv
1. Introduction	1
2. Experiment	2
2.1 Detector Fabrication	2
2.2 Detector Characterization	4
3. Results	5
3.1 I-V Characteristics	5
3.2 Barrier Height	7
3.3 X-ray Measurements	7
4. Conclusions	8
References	10
Acronyms	12
Distribution List	13

List of Figures

Figure 1. SI GaAs Schottky single detector with metal (a) Schottky and (b) ohmic contacts.....	3
Figure 2. SI GaAs wafer with (a) ohmic contacts on the back side and (b) Schottky contacts on the front side	4
Figure 3. Schematic diagram of X-ray tube configuration.	5
Figure 4. Current versus reverse voltage for detectors A, B, and C.	6
Figure 5. X-ray photocurrent measurements for detector C with 150 keV X-ray radiation under dark and with X-ray with a detector size of 2×2 mm.	8

List of Tables

Table 1. Important semiconductor properties for X-ray detectors.....	1
--	---

1. Introduction

Ideally, for X-ray detection, one requires materials of a high atomic number (Z) with a bandgap of about 1.5 eV, which is large enough to lower the electronic noise and small enough to allow charge carriers to recombine and produce a maximum number of electron-hole pairs.

Semiconductor materials with high mobility and lifetime are preferable. Among a few materials that fulfill these requirements are gallium-arsenic (GaAs) and cadmium-zinc-tellurium (CdZnTe or CZT). They are viable alternative to silicon (Si) or germanium (Ge) for the detection of X-rays above a few keV. GaAs and CZT are two of the compound semiconductors with a bandgap of ~ 1.5 eV, which is high enough to permit room temperature operation. The atomic number of GaAs and CZT's constituents are greater than or equal to that of Ge and have the advantages of a Ge detector, such as high detection efficiency and robustness.

Another requirement for X-ray detection is having a thick absorber layer with a low enough free carrier concentration. CZT detectors exhibit a charge collection efficiency closer to 1 with a good energy resolution even for photons of low energies (1). However, the major problems with CZT are low material yield, high cost, and non-uniformity. CZT detectors contains a large concentration of defects (2, 3), and hence, present a reduction of the electric field due to charge trapping on defects. They also present afterglow effects due to transient currents, caused during the equilibrium of charge distribution of the defect levels (4).

CZT is not suited for high flux operations, but is being used for lower flux applications like Positron Emission Tomography (PET) scanners or other applications where the X-ray energy is high, >20 keV. Si-based detectors have a low detection probability in comparison with GaAs since the photoelectric conversion efficiency scales with the atomic number of the detection system. Important semiconductor properties required for X-ray detectors are recorded on table 1.

Table 1. Important semiconductor properties for X-ray detectors.

Property	Units	Si	Ge	GaAs	SiC	CZT
Atomic number		14	32	31/33	14/12	48/30/52
Atomic weight		28.09	72.59	144.63	40	306.01
Density	gm/cm ³	2.33	5.33	5.32	3.21	
Bandgap (room temperature)	eV	1.12	0.66	1.42	3.0	1.548 for Zn = 0.06
Average energy per e-h pair	eV	3.65	2.85	4.2	~ 8.5	
Electron mobility, μ_e	cm ² /Vs	1500	3900	8500	~ 1000	
Hole mobility, μ_h	cm ² /Vs	450	1900	400	~ 100	
Minority carrier lifetime	s	2.5×10^{-3}	10^{-3}	$\sim 10^{-8}$	$\sim 10^{-6}$	
Intrinsic resistivity	Ω cm	2.3×10^5	47	10^8	$> 10^{12}$	10^9
Intrinsic carrier concentration	cm ⁻³	1.45×10^{10}	2.5×10^{13}	1.8×10^6	10^{-6}	$\sim 10^{15}$

NOTE: e-h = electron-hole and SiC = silicon-carbon.

Considering atomic weight as the most important factor, we realize that CZT is the best material for X-ray detection; however, thick good quality CZT material is difficult to produce and is very expensive. Hence, the alternative material is GaAs, because Ga and As have the high atomic numbers needed to be considered for X-ray detection and GaAs is well suited for low energy medical uses like dental X-ray and mammography. The processing and fabrication technology for GaAs is standard and the material can be obtained in large sizes (5). The Ga and As atomic numbers of 31 and 33, respectively, ensure sufficient detection efficiency for hard X-rays. A bandgap of 1.42 eV allows GaAs detectors to operate at room temperature, while the high-charge carrier mobilities of 8000 and $400 \text{ cm}^2 \text{ V}^{-1} \text{ S}^{-1}$ for electrons and holes, respectively, resulting in the high drift velocities at low electric field necessary for efficient operation. Considering all these factors, GaAs is a very promising material for radiation detections for imaging applications.

The main reported limitations of the spectroscopic performance of semi-insulated (SI) GaAs detectors are related to the shot noise created by the reverse current of the detector and the noise stimulated by the carrier trappings (6). However, medium, or even higher, performance can be attained with currently available SI GaAs materials.

This work deals with the fabrication of SI GaAs wafers with front and back end processing for Schottky and ohmic contacts. The front and back processing allows the pixilation on the underside, which can be flip chip bonded to printed circuit boards (PCB) or other suitable substrates, thereby making the interconnect easy for a two-dimensional array. A higher breakdown voltage will enhance the charge collection efficiency in these detectors. Fabrication was performed using commercially available 4 in. SI GaAs wafers. Fabricated wafers were diced to obtain single detectors of various sizes. Detectors were characterized for current-voltage (I-V) and X-ray radiation using appropriate electronic amplification. The data were analyzed and are presented here.

2. Experiment

2.1 Detector Fabrication

The detectors were fabricated from low dislocation density bulk 4 in. SI GaAs grown by the Vertical Bridgeman method, developed by AXT, Inc., with a resistivity of about $6.9 \times 10^7 \Omega \text{ cm}$ and a Hall mobility of $6395 \text{ cm}^2 \text{ V}^{-1} \text{ s}^{-1}$ at room temperature. The thickness was measured to be $520 \mu\text{m}$. The detectors were processed by an extremely difficult, labor intensive, front/back side process using five different photomasks. Figure 1 shows the cross section of the SI GaAs Schottky single detector used for the characterization. After the degreasing process, the wafer

was deoxidized by hydrochloric acid: de-ionized water (10:1) for a minute. The wafer was dried and loaded on to the Plasma Therm 790 plasma chemical vapor deposition (PECVD) and 0.25 μm thick silicon nitride was deposited as a passivation layer on the front side.

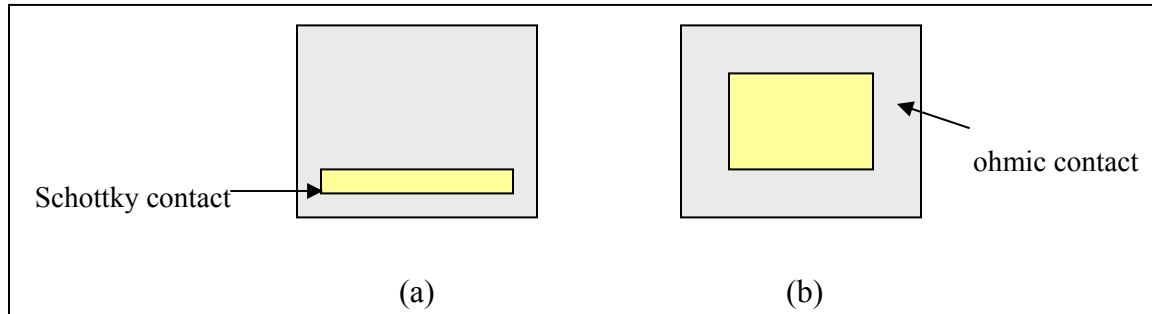


Figure 1. SI GaAs Schottky single detector with metal (a) Schottky and (b) ohmic contacts.

The retrieved wafer was cleaned in organic solvents and negative photolithographic techniques were used with mask 1 to impart a pattern on the back side. The wafer was dipped in a $5\%\text{H}_2\text{SO}_4 + 10\%\text{NH}_4\text{OH} + \text{H}_2\text{O}$ solution for 20 s prior to loading onto the e-beam evaporator. For ohmic contact, Ge/Au/Ni/Au was deposited followed by a lift-off process. To obtain low contact resistivity, the wafer was annealed in nitrogen. The wafer was cleaned and a 0.25 μm thick silicon nitride was again deposited on the back side just over the ohmic contact. Photolithographic techniques were used again with a positive mask to open up windows on the silicon nitride. Oxygen plasma was used in the March Reactive Ion Etching (RIE) system to open windows on the silicon nitride layer. The remaining photoresist was stripped off and the wafer was ashed and cleaned thoroughly. Another photolithographic process was done on the front side on the silicon nitride passivation layer followed by dry etching to open up windows. The remaining photoresist was cleaned away by standard techniques, and this was followed by negative resist photolithography.

A Karl Suss MA/BA6 mask aligner was used for back alignment using infrared cameras to make sure correspondence existed between front and back patterns for the Schottky devices. Schottky contact metals Ti and Au were deposited, lift-off was performed, and the wafer was thoroughly cleaned. Subsequently, a 0.25 μm thick silicon nitride was deposited to isolate the contacts and to lithographically open up windows. Dry etching was done to open windows, all the remaining photoresist was removed by stripping, and the wafer was cleaned thoroughly prior to dicing.

Figure 2 shows the pictures of the SI GaAs wafer with (a) ohmic contacts on the back side and (b) Schottky metal contacts on the front side. This front and back side processing allows the pixilation on the under side, which can be flip chip bonded to PCB or a suitable substrate, thereby making the interconnect easy for a two-dimensional array.

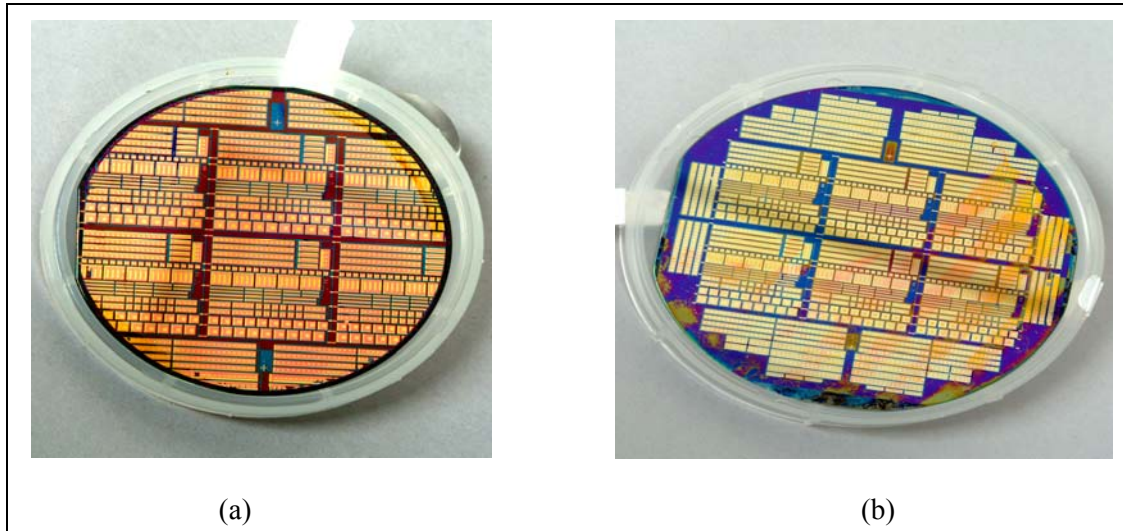


Figure 2. SI GaAs wafer with (a) ohmic contacts on the back side and (b) Schottky contacts on the front side

2.2 Detector Characterization

The fabricated wafer was diced to obtain individual detectors for electrical characterization and X-ray detection measurements. All the I-V measurements were done using an HP 4150 parametric analyzer. For the experiments, we used $2 \times 2 \text{ mm}^2$ Schottky detectors mounted on a leadless chip carrier (LCC) with the ohmic side touching the LCC surface. Metal wires were bonded to the Schottky contact pads and the LCC surface for ohmic contact. All I-V measurements were performed at room temperature.

For the X-ray detection, a continuous source, a Norelco MG300 X-ray tube, was used, which is an industrial tube originally designed for radiography applications. The applied voltage between the anode and cathode can be varied between 120 and 300 kV. The maximum current available at 300 kV is 10 mA. The electrons are emitted from a heated wound wire filament. The full voltage appears across the anode-cathode gap, accelerating the electrons towards the tungsten (W) anode target. The electrons are stopped in the W target and in stopping/de-accelerating produce a broad spectrum of X-rays known as bremsstrahlung.

The X-ray geometry is shown in figure 3 and indicates an incident electron beam hitting the tungsten-copper (W-Cu) anode converter plate (99.5%W, 0.5%Cu). The target is oriented at an angle of 68° with respect to the incident electron beam axis. The output window is oriented 90° with respect to the electron beam incident on the W target. Electrons with the assigned endpoint energy hit a W target.

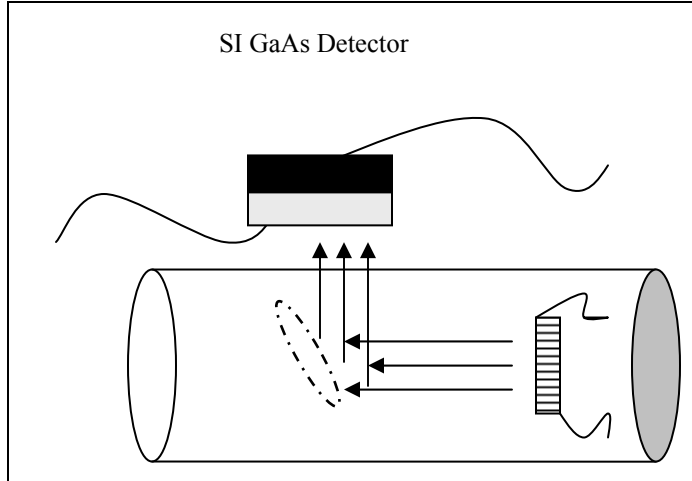


Figure 3. Schematic diagram of X-ray tube configuration.

The velocity of the electrons is changed, or in the extreme case, the electrons are stopped by the heavy nucleus of the tungsten. In de-accelerating, photons are emitted in the X-ray part of the electromagnetic spectrum (~ 300 eV to 300 keV). The spectrum of X-rays is broad but peaked at approximately $\frac{1}{4}$ of the endpoint energy (applied voltage). The flux of electrons through a 1 cm thick layer of air located just outside the window is counted. In this experiment, the endpoint energy was 150 kV.

3. Results

3.1 I-V Characteristics

The reverse bias leakage current density for three different diodes (A, B, and C) are measured and used for current density calculations. The I-V measurements were performed at room temperature up to a reverse bias of 1000 V. In the case of detectors A and B, the breakdown voltage is between 600–800 V; whereas, in the case of C, even after 1000 V, there is no indication of breakdown. We used the definition of breakdown voltage as the voltage measured at a specified current in the electrical breakdown region of a semiconductor diode. Electrical breakdown is a large, usually abrupt, rise in electric current in the presence of a small increase in voltage. As the reverse bias increased from 0 to -1000 V, the reverse bias current changed from -2 nA at 20 V and -650 nA at 1000 V for detector A, with breakdown occurring at around 800 V. The same occurred for detector B: -1.8 nA at 20 V and -1180 nA for 1000 V, with the breakdown around 600 V. In the case of detector C, the breakdown voltage couldn't be seen to change much as was observed in detectors A and B. The observed current was -1.6 nA for 20 V and -6.7 nA at 1000 V. These observed leakage currents for a 0–1000V reverse bias are significantly better than similarly fabricated detectors of same size and geometry. In one case, Baldini et al. (6) reported the leakage current changing from 10^{-8} to 10^{-4} A for SI GaAs detectors

for reverse bias of 0–600 V for different levels of dopant concentration. Jayavel et al. (7) reported leakage current in the neighborhood of 250 nA for 50 μm thick SI-GaAs for a reverse voltage of 60 V. Sellin et al. (8) reported an epitaxial 270 μm GaAs layer grown on to an n-type GaAs wafer of thickness 270 μm acting as a substrate; they obtained a leakage current in around 7 μA for a reverse bias of 70 V. In our case, the lower leakage current and higher breakdown voltage were obtained because of the good quality of the SI GaAs crystal with lower defects. Low leakage current is also indicative of good metal contacts and negligible contamination during processing. The measured current is plotted in figure 4.

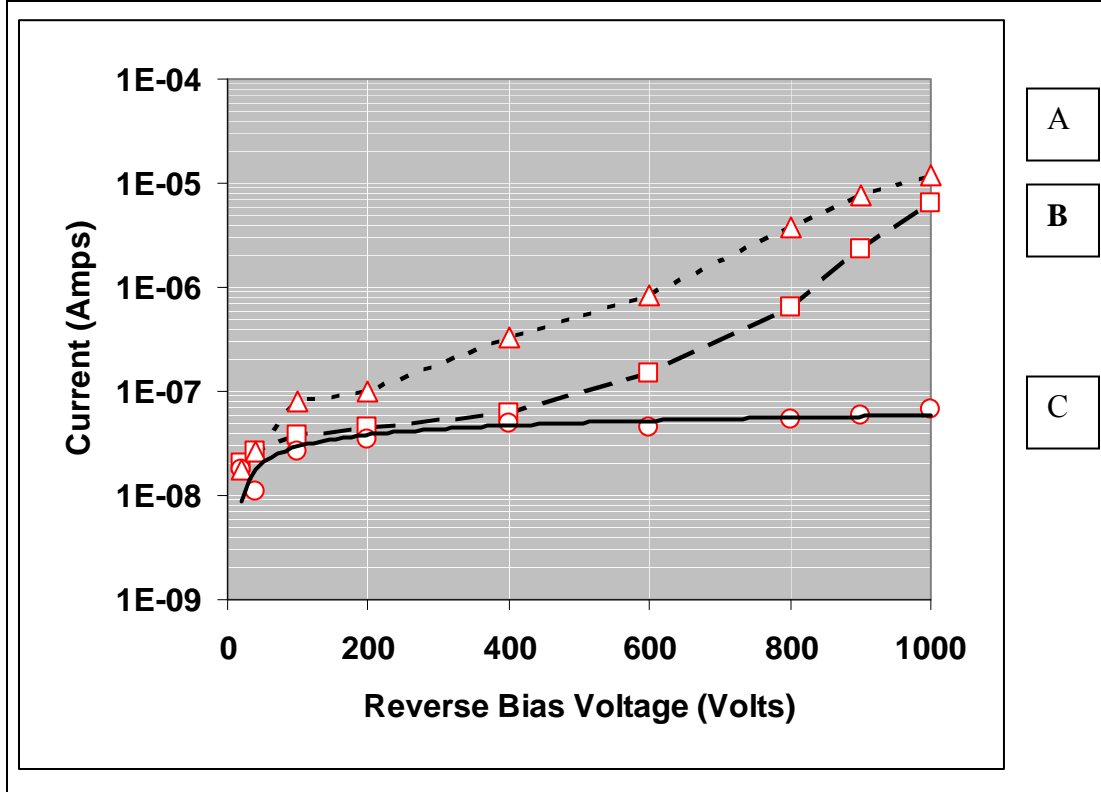


Figure 4. Current versus reverse voltage for detectors A, B, and C.

As can be seen in the figure 4, we obtained high breakdown voltage at least in two cases. The breakdown voltages for detector A and B are between 600–800 V. We couldn't obtain the breakdown voltage for detector C, which seems to be beyond 1000 V. The reverse breakdown voltage of these front and back side processed SI GaAs Schottky detectors A, B, and C is much higher than what we have seen in literature. Schwarz et al. (9) reported for a breakdown reverse bias voltage close to 250 V X-ray imaging detectors. Paolo Rossi et al. (10) fabricated and characterized SI-GaAs detectors for medical imaging and they observed reverse breakdown voltages increasing with decreasing size of the Schottky pads. They obtained a breakdown of 220 V for a pad size of 1 mm.

The higher breakdown voltages in the detectors we have fabricated have many advantages. It gives the benefit of depleting the entire thickness of the wafer, which greatly improves the charge collection efficiency. Also, the larger thickness of the detector being depleted means that the stopping power is higher, which makes the detector better suited for the high energy of X-ray detection.

3.2 Barrier Height

To further understand the metal semiconductor contacts in the SI-GaAs Schottky diodes, we calculated the barrier height, which depends upon the metal work function and the surface states of the semiconductor. The relationship between the current and applied voltage from the thermionic equation is given by the following (10, 11):

$$I = I_s \left[\exp\left(\frac{qV}{nk_b T}\right) - 1 \right] \quad (1)$$

where

$$I_s = A^{**} T^2 \exp\left(\frac{-q\phi_B}{k_B T}\right) \quad (2)$$

and

$$\phi_B = \frac{k_B T}{q} \ln\left(\frac{A^{**} T^2}{I_s}\right). \quad (3)$$

where I is the measured current (A) in these equations; I_s is the saturation current (A); A^{**} is the Effective Richardson constant $8.6 \text{ A cm}^{-2} \text{ K}^{-2}$ for n-; GaAs. V is the applied voltage; T is the absolute temperature (K); n is the ideality factor; k_B is the Boltzmann constant $1.38 \times 10^{-23} \text{ J K}^{-1}$; and ϕ_B is the barrier height (eV).

Using equation 3, we calculated the zero-bias barrier height for detectors A, B, and C and found it to be 0.95, 0.86, and 0.86 eV, respectively, at room temperature. This value is comparable to calculated barrier height with Au metal contacts on GaAs Schottky detectors (12). Additional calculation of the ideality factor and barrier height under different temperature is being performed and will be published elsewhere.

3.3 X-ray Measurements

The X-ray photocurrent of the GaAs detectors was determined using the 150 keV, 3 mA X-ray radiation shining on the detectors. The photocurrent under exposed X-ray shows the photocurrent without much variation from 0–1000 V reverse bias. For any given voltage, the photocurrent change from nano amps to micro amps shows an increase of three orders of magnitude, indicating the high quality performance of the detector. Detector C has a dark current of about 20 nA for a voltage range starting at a reverse voltage of 20 V to 900 V. This dark current remains the same until it reaches its breakdown voltage. Under the exposure of X-

ray beam of 150 KeV at 3 mA, the photocurrent jumps to about 2 μA , which remain the same for same voltage as the previous measurement. This indicates that the detector is very sensitive to X-ray exposure and the detectivity is extremely good. A very similar response can be seen in the case of detector B under the same X-ray exposure. The reverse bias photocurrent is plotted in log scale on figures 5 and 6 for detectors A and B, respectively. The photocurrent was found to be about $5\mu\text{A}/\text{cm}^2$ in both detectors and was consistent in both cases for the reverse bias of 0–800 V. No attempt was made to characterize these detectors under various X-ray energy levels.

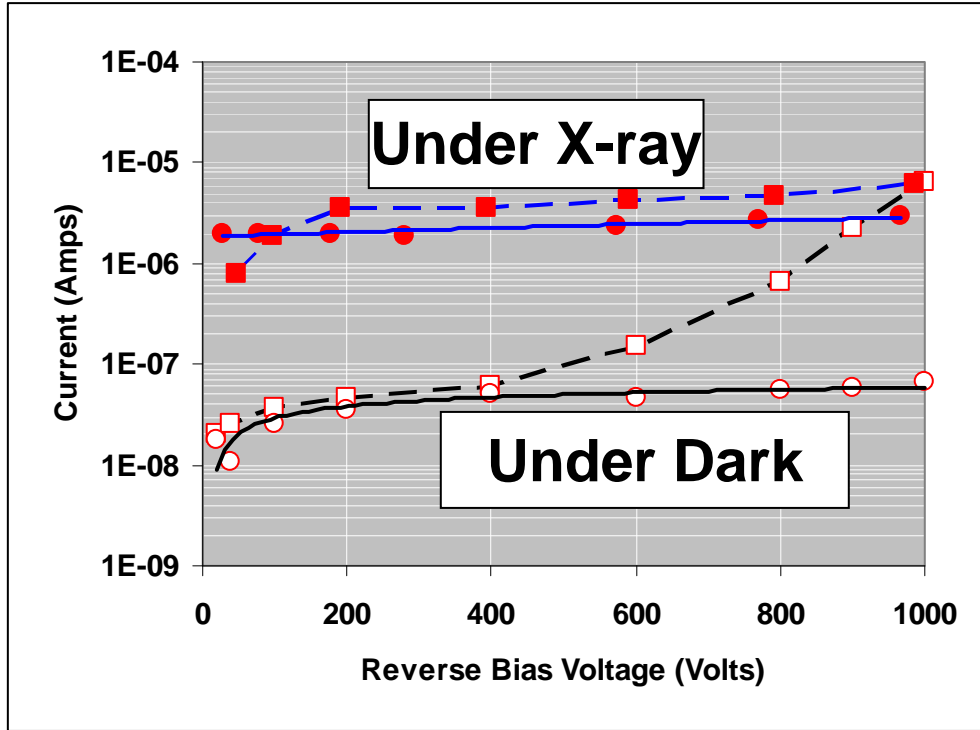


Figure 5. X-ray photocurrent measurements for detector C with 150 keV X-ray radiation under dark and with X-ray with a detector size of 2×2 mm.

NOTE: The solid lines are for detector C and dashed lines are for detector B.

4. Conclusions

SI GaAs Schottky detectors were fabricated using front and back side photolithographic processing with Ti/Au for Schottky and Ge/Au/Ni/Au for ohmic contacts. In a number of detectors tested, the breakdown voltage reached close to 600–800 V, and in one case, the breakdown voltage was beyond 1000 V reverse bias. In the characterized detectors, the leakage current was found to be between 2–90 nA until the breakdown voltage was reached. This low leakage current is indicative of the quality of the material, processing, and fabrication of the devices. The calculated barrier height was found to be 0.95, 0.86, and 0.86 eV, respectively, for the three detectors under consideration, and they compared well with similar diodes. These

detectors were characterized with 150 keV, 3 mA X-ray radiation under dark conditions and they responded well by showing more than a hundred fold increase in photocurrent due to production of e-h pairs by the ionization processes. The high breakdown voltage in these detectors will enhance the charge collection efficiency. In addition, thicker samples can be used with high breakdown voltage, which will provide higher stopping power, thus making these detectors suitable for high energy X-ray detection.

References

1. Macri, J.R.; Boykin, D.V.; Larson, K.; Mayer, M.; McConnell, M.L.; Ryan, J.M.; Cherry, M.L.; Guzik, T.G.; Apotovsky, B.A.; Butler, J.F.; Doty, F.P.; Lingren, C.L. Progress in Development of Large Area Sub-millimeter Resolution CdZnTe Strip Detectors. *Proceedings from SPIE* 1996, 2859, 29.
2. Verger, L.; Bonnefoy, J.P.; Glasser, F.; Ouvrier-Buffet, P. New developments in CdTe and CdZnTe detectors for X and gamma – ray applications. *J. Electronics Mater.* **1996**, 26, 738.
3. Compound Semiconductors. http://www.rssd.esa.int/stj/STJ_compound.html (September 2007).
4. Lumb, D.H.; Owens, A.; Bavdaz, M.; Peacock, T. Development of compound semiconductor detectors at ESA. <http://sci.esa.int/science-e/www/object/doc.cfm?fobjectid=39663> (accessed September 2007).
5. Bates, R.L.; Manolopoulos, S.; Mathieson, K.; Meikle, A.; O'Shea, V.; Raine, C.; Smith, K.M.; Watt, J.; Whitehill, C.; Pospíšil, S.; Wilhem, I.; Doležal, Z.; Juergensen, H.; Heuken, M. Development of low-pressure vapour-phase epitaxial GaAs for medical imaging. *Nuclear Instruments and Methods in Physics Research A* **1999**, 434 (1).
6. Baldini, R.; Vanni, P.; Nava, F.; Canali, G.; Lanzieri, C. Influence of substrate on the performance of semi-insulating GaAs detectors. *Nuclear Instruments and Methods in Physics Research A* **2000**, 449, 268.
7. Jayavel, P.; Ghosh, S.; Jhingan, A.; Avasthi, D.K.; Asokan, K.; Kumar, J. Study of the performance of SI-GaAs and Si-InP surface barrier detectors for alpha and gamma detection. *Nuclear Instruments and Methods in Physics Research A* **2000**, 454, 252.
8. Sellin, P.J.; El-Abbassi, H.; Rath, S.; Bourgoin, J.C.; Sun, G.C. Performance of epitaxial GaAs radiation detectors grown by vapour-based chemical reaction. *Nuclear Instruments and Methods in Physics Research A* **2003**, 512, 433.
9. Schwarz, C.; Campbell, M.; Goeppert, R.; Heijne, E.H.M.; Ludwig, J.; Meddeler, G.; Mikulec, B.; Pernigotti, E.; Rogella, M.; Runge, K.; Söldner-Rembold, A.; Smith, K.M.; Snoeys, W.; Watt, J. X-ray imaging using a hybrid photon counting GaAs pixel detector. *Nuclear Physics B* **1999**, 78, 491.
9. Russo, P.; Mettivier, G. Characterization of 600- μm thick SI-GaAs detectors for medical imaging. *Nuclear Instruments and Methods in Physics Research A* **2001**, 466, 79.

10. Rhoderick, E.H.; Williams, R.H. *Metal – Semiconductor Contacts*, 2nd ed.; Oxford Clarendon: London, United Kingdom, 1988, pp 51–3.
11. Sze, S.M. *Physics of Semiconductor Devices*, 2nd ed.; Wiley: New York, NY, 1981, pp 256–263.
12. Biber, M.; Temirci, C.; Türüt, A. Barrier height enhancement in the Au/n-GaAs Schottky diodes with anodization process. *J. Vac. Sci. Technol. B* **2002**, *20* (1), 10.

Acronyms

As	arsenic
Au	gold
CdZnTe or CZT	cadmium-zinc-tellurium
e-h	electron-hole
Ga	gallium
GaAs	gallium-arsenic
Ge	germanium
I-V	current-voltage
LCC	leadless chip carrier
Ni	nickel
PCB	printed circuit boards
PECVD	plasma chemical vapor deposition
PET	Positron Emission Tomography
RIE	Reactive Ion Etching
SI	semi-insulated
Si	silicon
SiC	silicon-carbon
W	tungsten
W-Cu	tungsten-copper

Distribution List

Copies Organization

57 US ARMY RSRCH LAB
 ATTN AMSRD ARL SE EE T ALEXANDER
 ATTN AMSRD ARL SE EI J LITTLE
 ATTN AMSRD ARL CI OK T
 TECHL PUB (2 copies)
 ATTN AMSRD ARL CI OK TL
 TECHL LIB (2 copies)
 ATTN AMSRD ARL D J M MILLER
 ATTN AMSRD ARL SE DE K BLAINE
 ATTN AMSRD ARL SE DE M LITZ
 ATTN AMSRD ARL SE DP A LELIS
 ATTN AMSRD ARL SE DP B MORGAN
 ATTN AMSRD ARL SE E G WOOD
 ATTN AMSRD ARL SE E H POLLEHN
 ATTN AMSRD ARL SE E L BLISS
 ATTN AMSRD ARL SE E T BOWER
 ATTN AMSRD ARL SE E0 N FELL
 ATTN AMSRD ARL SE EE B ZANDI
 ATTN AMSRD ARL SE EE K ALIBERTI
 ATTN AMSRD ARL SE EE N GUPTA
 ATTN AMSRD ARL SE EI D BEEKMAN
 ATTN AMSRD ARL SE EI G BRILL
 ATTN AMSRD ARL SE EI J GOMATHAM
 ATTN AMSRD ARL SE EI K K CHOI
 ATTN AMSRD ARL SE EI K OLVER
 ATTN AMSRD ARL SE EI N DHAR
 ATTN AMSRD ARL SE EI P FOLKES
 ATTN AMSRD ARL SE EI P TAYLOR
 ATTN AMSRD ARL SE EI
 P WIJEWAMASURIYA
 ATTN AMSRD ARL SE EI R TOBER
 ATTN AMSRD ARL SE EI W BECK
 ATTN AMSRD ARL SE EI W SARNEY
 ATTN AMSRD ARL SE EI Y CHEN
 ATTN AMSRD ARL SE EM F SEMENDY
 ATTN AMSRD ARL SE EM G DANG
 ATTN AMSRD ARL SE EM G GARRETT
 ATTN AMSRD ARL SE EM G SIMONIS
 ATTN AMSRD ARL SE EM M REED
 ATTN AMSRD ARL SE EM
 M TAYSING LARA
 ATTN AMSRD ARL SE EM N BAMBHA
 ATTN AMSRD ARL SE EM N DAS
 ATTN AMSRD ARL SE EM P SHEN
 ATTN AMSRD ARL SE EM W CHANG
 ATTN AMSRD ARL SE R P AMIRTHARAJ
 ATTN AMSRD ARL SE RE A DARWISH
 ATTN AMSRD ARL SE RE C FAZI

Copies Organization

US ARMY RSRCH LAB (cont'd)
 ATTN AMSRD ARL SE RL
 A WICKENDEN
 ATTN AMSRD ARL SE RL D EWING
 ATTN AMSRD ARL SE RL E ZAKAR
 ATTN AMSRD ARL SE RL J COSTANZA
 ATTN AMSRD ARL SE RL K JONES
 ATTN AMSRD ARL SE RL M DERANGE
 ATTN AMSRD ARL SE RL M DUBEY
 ATTN AMSRD ARL SE RL P SHAH
 ATTN AMSRD ARL SE RL S KILPATRICK
 ATTN AMSRD ARL SE RL S SVENSSON
 ATTN AMSRD ARL SE EP M WRABACK
 ATTN IMNE ALC IMS MAIL & RECORDS
 MGMT
 ADELPHI MD 20783-1197

1 ADMNSTR
 DEFNS TECHL INFO CTR
 ATTN DTIC OCP (ELECTRONIC COPY)
 8725 JOHN J KINGMAN RD STE 0944
 FT BELVOIR VA 22060-6218

1 US ARMY RSRCH LAB
 ATTN AMSRD ARL CI OK TP
 TECHL LIB T LANDFRIED
 BLDG 4600
 APG MD 21005-5066

1 S SINGH
 PO BOX 88
 GLENDALE MD 20769

1 DIRECTOR
 US ARMY RSRCH LAB
 ATTN AMSRD ARL RO EV W D BACH
 PO BOX 12211
 RESEARCH TRIANGLE PARK NC 27709

TOTAL 1 elec, 61 HCs

INTENTIONALLY LEFT BLANK.